articles

molecular pharmaceutics

Iodinated NanoClusters as an Inhaled Computed Tomography Contrast Agent for Lung Visualization

Kristin L. Aillon,[†] Nashwa El-Gendy,[†,‡] Connor Dennis,[||] Jeffrey P. Norenberg,[†,‡] Jacob McDonald,[§] and Cory Berkland*[,†,||]

Department of Pharmaceutical Chemistry, University of Kansas, Lawrence Kansas 66047, Department of Pharmaceutics and Industrial Pharmacy, Faculty of Pharmacy, Beni-Suef University, Beni-Suef, Egypt, Lovelace Respiratory Research Institute, Albuquerque, New Mexico 87115, Department of Chemical and Petroleum Engineering, University of Kansas, Lawrence, Kansas 66047, and Department of Pharmacy Practice, College of Pharmacy, University of New Mexico Health Sciences Center

Received March 16, 2010; Revised Manuscript Received June 21, 2010; Accepted June 24, 2010

Abstract: Improvements to contrast media formulations may be an effective way to increase the accuracy and effectiveness of thoracic computed tomography (CT) imaging in disease evaluation. To achieve contrast enhancement in the lungs, a relatively large localized concentration of contrast media must be delivered. Inhalation offers a noninvasive alternative to intrapleural injections for local lung delivery, but effective aerosolization may deter successful imaging strategies. Here, NanoCluster technology was applied to N1177, a diatrizoic acid derivative, to formulate low density nanoparticle agglomerates with aerodynamic diameters ≤ 5 μm. Excipient-free N1177 NanoCluster powders were delivered to rats by insufflation or inhalation and scanned using CT up to 1 h post dose. CT images after inhalation showed a $\sim$120 (HU) Hounsfield units contrast increase in the lungs, which was more than sufficient contrast for thoracic CT imaging. Lung tissue histology demonstrated that N1177 NanoClusters did not damage the lungs. NanoCluster particle engineering technology offers a novel approach to safely and efficiently disseminate high concentrations of contrast agents to the lung periphery.

Keywords: NanoCluster; contrast agent; particle engineering; CT imaging; N1177; aerosol

Introduction

Thoracic computed tomography (CT) imaging has been widely used for visualization of soft tissues in the chest, primarily the heart and lungs. For lung damage and disease, CT is considered a noninvasive technique for 3D imaging of tumor size and staging in lung cancer,[1−3] for chest injuries and abnormalities in lung size and position,[1] and for determination of fluid collection in diseases such as pneumonia and cystic fibrosis.[4] The success of CT imaging in disease diagnosis depends primarily on imaging accuracy. During lung cancer prognosis, false positive results can lead to unnecessary and costly further testing.[5] Although several advancements have been made to imaging techniques, challenges still remain to further increase imaging accuracy. Along with advancing imaging instrumentation, inaccuracy

* Corresponding author. University of Kansas, 2030 Becker Drive, Lawrence, KS 66047. Phone: (785) 864-1455. Fax: (785) 864-1454. E-mail: berkland@ku.edu.

[†] Department of Pharmaceutical Chemistry, University of Kansas.

[‡] Beni-suef University.

[§] Lovelace Respiratory Research Institute.

[||] Department of Chemical and Petroleum Engineering, University of Kansas.

(1) Brown, L. R.; Muhm, J. R. Computed tomography of the thorax. Current perspectives. *Chest* **1983**, *83*, 806–813.

(2) Islam, T.; Harisinghani, M. G. Overview of nanoparticle use in cancer imaging. *Cancer Biomarkers* **2009**, *5*, 61–67.

(3) Rutten, A.; Prokop, M. Contrast agents in x-ray computed tomography and its application in oncology. *Anti-Cancer Agents Med. Chem.* **2007**, *7*, 307–316.

(4) Robinson, T. E. Computed tomography scanning techniques for the evaluation of cystic fibrosis lung disease. *Proc. Am. Thorac. Soc.* **2007**, *4*, 310–315.

(5) Verschakelen, J. A.; De Wever, W.; Bogaert, J. Role of computed tomography in lung cancer staging. *Curr. Opin. Pulm. Med.* **2004**, *10*, 248–255.

10.1021/mp1000718
Published on Web 06/24/2010

challenges could be met through the development of improved contrast media strategies.

Several compounds have been identified as capable of providing contrast enhancement in CT imaging. By far, the most common contrast agent is barium sulfate. Suspensions of insoluble barium sulfate are delivered orally for imaging the gastrointestinal tract. However, for thoracic imaging, barium sulfate is contraindicated as studies have suggested that barium sulfate can cause granulomas and asphyxiation and could potentially be fatal.[6,7] Iodinated compounds, such as derivatives of diatrizoic acid, have proved to be safe and effective alternatives to barium sulfate as CT contrast agents.[3] There are several available iodinated contrast agents that are given as intravenous injections for thoracic CT imaging.[3] When given iv, however, these compounds are eliminated quickly from the body with insufficient amounts of compound localized to the lung. For lung visualization, large local concentration is needed to achieve the minimum of 30 Hounsfield units (HU) necessary for contrast enhancement.[8] Direct delivery may, therefore, be needed to concentrate contrast media to the lungs. For example, studies have shown that a >100 HU contrast can be achieved in regional lymph nodes after local delivery of iodinated contrast agents (sc or ip injection).[9,10]

Agents providing improved contrast must be efficiently delivered to increase imaging accuracy. To locally deliver contrast agents to the lungs, many studies have focused on intrapleural injection, which proves to be very invasive.[11,12] Inhalation provides a noninvasive alternative, if sufficient quantities can be delivered. Surprisingly, very few studies have focused on pulmonary delivery of contrast agents to the lungs.[8,13−17] This may be due to unsuccessful aerosolization of formulations resulting in low doses and insufficient dissemination to the lung periphery. The development of formulations with proper aerosol characteristics would facilitate successful strategies for noninvasive delivery of contrast agents to the lungs.

Recently, a controlled nanoparticle agglomeration process has been developed that resulted in particles with desirable characteristics for inhalation.[18−24] These NanoClusters have aerodynamic diameters between 1 and 5 μm, suggesting the powders are capable of deep lung deposition in the respiratory bronchioles and alveoli. 6-Ethoxy-6-oxohexyl-3,5-bis(acetylamino)-2,4,6-triiodobenzoate (N1177) is a water insoluble diatrizoic acid derivative that has recently exhibited macrophage uptake after iv injection in rabbits.[25−27] N1177 showed promise as an effective contrast agent in those studies and may translate well to lung visualization. The NanoCluster particle technology was applied to N1177 to improve aerosol entrainment, deposition, and access to the lung periphery.

(6) Buschman, D. L. Barium sulfate bronchography. Report of a complication. *Chest* **1991**, *99*, 747–749.

(7) Tamm, I.; Kortsik, C. Severe barium sulfate aspirationinto the lung: clinical presentation, prognosis and therapy. *Respiration* **1999**, *66*, 81–84.

(8) McIntire, G. L.; Bacon, E. R.; Toner, J. L.; Cornacoff, J. B.; Losco, P. E.; Illig, K. J.; Nikula, K. J.; Muggenburg, B. A.; Ketai, L. Pulmonary delivery of nanoparticles of insoluble, iodinated CT X-ray contrast agents to lung draining lymph nodes in dogs. *J. Pharm. Sci.* **1998**, *87*, 1466–1470.

(9) McIntire, G. L.; Bacon, E. R.; Illig, K. J.; Coffey, S. B.; Singh, B.; Bessin, G.; Shore, M. T.; Wolf, G. L. Time course of nodal enhancement with CT X-ray nanoparticle contrast agents: effect of particle size and chemical structure. *Invest. Radiol.* **2000**, *35*, 91–96.

(10) Wisner, E. R.; Katzberg, R. W.; Koblik, P. D.; Shelton, D. K.; Fisher, P. E.; Griffey, S. M.; Drake, C.; Harnish, P. P.; Vessey, A. R.; Haley, P. J.; et al. Iodinated nanoparticles for indirect computed tomography lymphography of the craniocervical and thoracic lymph nodes in normal dogs. *Acad. Radiol.* **1994**, *1*, 377–384.

(11) Liu, J.; Wong, H. L.; Moselhy, J.; Bowen, B.; Wu, X. Y.; Johnston, M. R. Targeting colloidal particulates to thoracic lymph nodes. *Lung Cancer* **2006**, *51*, 377–386.

(12) Medina, L. A.; Calixto, S. M.; Klipper, R.; Phillips, W. T.; Goins, B. Avidin/biotin-liposome system injected in the pleural space for drug delivery to mediastinal lymph nodes. *J. Pharm. Sci.* **2004**, *93*, 2595–2608.

(13) Videira, M. A.; Botelho, M. F.; Santos, A. C.; Gouveia, L. F.; de Lima, J. J.; Almeida, A. J. Lymphatic uptake of pulmonary delivered radiolabelled solid lipid nanoparticles. *J. Drug Targeing* **2002**, *10*, 607–613.

(14) Videira, M. A.; Gano, L.; Santos, C.; Neves, M.; Almeida, A. J. Lymphatic uptake of lipid nanoparticles following endotracheal administration. *J Microencapsulation* **2006**, *23*, 855–862.

(15) Szmigielski, W.; Klamut, M.; Siezieniewska, Z.; Chibowski, D.; Korobowicz, E.; Rubai, B.; Wolski, T.; Tynecka, Z. Powdered diatrizoic acid for radiography of the respiratory tract. Part I. experimental investigation. *Acta Radiol.* **1991**, *32*, 415–420.

(16) Szmigielski, W.; Klamut, M.; Dahniya, M.; Klonowski, S.; Furmanik, F.; Kupisz, K.; Mahdi, O. Powdered diatrizoic acid for radiography of the respiratory tract. Part II. clinical application. *Acta Radiol.* **1991**, *32*, 467–473.

(17) Ketai, L. H.; Muggenburg, B. A.; McIntire, G. L.; Bacon, E. R.; Rosenberg, R.; Losco, P. E.; Toner, J. L.; Nikula, K. J.; Haley, P. J. CT imaging of intrthoracic lymph nodes in dogs with bronchoscopically administered iodinated nanoparticles. *Acad. Radiol.* **1999**, *6*, 49–54.

(18) El-Gendy, N.; Berkland, C. Combination chemotherapeutic dry powder aerosols via controlled nanoparticle agglomeration. *Pharm. Res.* **2009**, *26*, 1752–1763.

(19) El-Gendy, N.; Gorman, E. M.; Munson, E. J.; Berkland, C. Budesonide nanoparticle agglomerates as dry powder aerosols with rapid dissolution. *J. Pharm. Sci.* **2009**, *98*, 2731–2746.

(20) Plumley, C.; Gorman, E. M.; El-Gendy, N.; Bybee, C. R.; Munson, E. J.; Berkland, C. Nifedipine nanoparticle agglomeration as a dry powder aerosol formulation strategy. *Int. J. Pharm.* **2009**, *369*, 136–143.

(21) Bailey, M. M.; Gorman, E. M.; Munson, E. J.; Berkland, C. Pure insulin nanoparticle agglomerates for pulmonary delivery. *Langmuir* **2008**, *24*, 13614–13620.

(22) Peek, L. J.; Roberts, L.; Berkland, C. Poly(D,L-lactide-*co*-glycolide) nanoparticle agglomerates as carriers in dry powder aerosol formulation of proteins. *Langmuir* **2008**, *24*, 9775–9783.

(23) Shi, L.; Plumley, C. J.; Berkland, C. Biodegradable nanoparticle flocculates for dry powder aerosol formulation. *Langmuir* **2007**, *23*, 10897–10901.

(24) El-Gendy, N.; Aillon, K. L.; Berkland, C. Dry powdered aerosols of diatrizoic acid nanoparticle agglomerates as a lung contrast agent. *Int. J. Pharm.* **2010**, *391*, 305–312.

In this study, an excipient-free NanoCluster formulation was developed for N1177. Particle size analysis and cascade impaction data suggested potential deposition of the NanoClusters in the parenchyma. Pulmonary delivery of N1177 NanoClusters to rats resulted in a ~120 HU contrast enhancement. Histological examination of lung tissue post inhalation showed no acute lung toxicity compared to normal lung tissue. Overall, the N1177 NanoClusters were successful in safely achieving enhanced lung visualization with contrast agent deposition in the lung periphery.

Materials and Methods

N1177 NanoCluster Fabrication. N1177 NanoCluster suspensions were formulated by milling 7 g of N1177 powder (generously provided from NanoScan Imaging, LLC.) in 200 mL of distilled water (Barnstead International EASYpure RODI system) for 2 h. A Netzsch MiniCer Media Mill (NETZSCH Fine Particle Technology) was operated using YTZ grinding media (0.5 mm, Tosoh Corp.) under an agitation speed of 2,700 rpm. Particle size of NanoCluster suspensions was determined by dynamic light scattering (Brookhaven Instruments Corp., ZetaPALS) at different time intervals during the milling process. After milling, the collected suspension was frozen at −80 °C and freeze-dried (Labconco FreeZone 1). Drying lasted ~36 h to remove all appreciable water content. Lyophilized NanoCluster powder was stored in glass bottles at room temperature for further use.

Particle Size and Morphology by Scanning Electron Microscopy (SEM). The size and morphology of the lyophilized N1177 NanoCluster powder were evaluated using an LEO 1550 field emission scanning electron microscope and compared to that of N1177 powder as received. Prior to imaging, the samples were sputter-coated with gold for 3 min.

Chemical Stability by HPLC−UV. N1177 chemical stability during NanoCluster formulation was determined by chromatographic analysis of N1177 NanoClusters compared to N1177 powder as received. The HPLC−UV system consisted of a Shimadzu CBM-20A system controller, LC-10AT solvent delivery pump, SPD-10A UV detector, and SIL-10AxL autoinjector. Chromatograms were acquired and analyzed using Shimadzu Class vp 7.4 software. A Kromasil C18 column (100 × 4.6 mm) was used for separation. An isocratic system was used with a mobile phase of 65/35 ammonium acetate (25 mM, pH 4.0)/acetonitrile at a flow rate of 1.0 mL/min, and detection was performed at 240 nm. Samples of N1177 NanoClusters and powder as received were made at concentrations of 50 μg/mL in acetonitrile, and 50 μL of sample was injected on the system. Percent degradation was determined using the peak area of the degradant relative to the N1177 peak area.

Thermal Analysis by Differential Scanning Calorimetry. The effect of the NanoCluster process on the crystalline state was determined by differential scanning calorimetry (DSC). Curves of N1177 NanoClusters and powder as received were collected on a Q100 DSC (TA Instruments). Samples (~2.5 mg) were loaded into aluminum hermetic pans. Samples were run from 25 to 250 °C heating at 10 °C/min under dry nitrogen at 50 mL/min. Curves were analyzed with Universal Analysis 2000 (version 4.3A) software (TA Instruments).

Particle Stability. The particle stability of the NanoClusters was determined by measuring the particle size of N1177 NanoCluster suspensions subjected to homogenization. Approximately 1 mg of powder was suspended in Pluronic-F127 (BASF) (1 μg/mL) or 1,2-dipalmitoyl-*sn*-glycero-3-phosphocholine (DPPC; Sigma-Aldrich) (13.25 mg/mL), which was used to mimic lung surfactant. The particle size of the suspensions was measured by dynamic light scattering. The suspensions were diluted with Pluronic-F127, DPPC, or water until measurable by the DLS instrument. The suspensions were then subjected to low speed homogenization (5,000 rpm) for 15 s and then high speed homogenization (25,000 rpm) for 15 s with particle size measurements taken after each. Statistical analysis was performed by a *t*-test at the 95% confidence level.

Aerodynamic Size Distribution by Time-of-Flight Analysis. The aerodynamic size distribution of the N1177 NanoCluster powder was determined by a time-of-flight instrument (Aerosizer; Amherst Process Instruments, Inc.). Approximately 1 mg of powder was placed in the instrument disperser, and particle size measurements were acquired over 60 s under high shear and feed rate. The instrument size limits were 0.10−200 μm, and particle counts were above 100,000 for all measurements.

Aerosol Characterization by Cascade Impaction. Aerodynamic characteristics of the N1177 NanoClusters as compared to N1177 powder as received were analyzed using an Ambient Cascade Impactor (Tisch Environmental, Inc.). Approximately 10 mg of powder on a piece of weighing paper was introduced manually to the mouthpiece of the impactor, which was operated at ~30 L/min. The cutoff particle aerodynamic diameters for each impactor stage were as follows: preseparator (10.0 μm), stage 0 (9.0 μm), stage 1 (5.8 μm), stage 2 (4.7 μm), stage 3 (3.3 μm), stage 4 (2.1 μm), stage 5 (1.1 μm) stage 6 (0.7 μm), stage 7 (0.4 μm) and filter (0.0 μm). Powder deposited on each impactor stage

(25) Hyafil, F.; Cornily, J. C.; Feig, J. E.; Gordon, R.; Vucic, E.; Amirbekian, V.; Fisher, E. A.; Fuster, V.; Feldman, L. J.; Fayad, Z. A. Noninvasive detection of macrophages using a nanoparticulate contrast agent for computed tomography. *Nat. Med.* **2007**, *13*, 636–641.

(26) Hyafil, F.; Cornily, J. C.; Rudd, J. H.; Machac, J.; Feldman, L. J.; Fayad, Z. A. Quantification of inflammation within rabbit atherosclerotic plaques using the macrophage-specific CT contrast agent N1177: a comparison with 18F-FDG PET/CT and histology. *J. Nucl. Med.* **2009**, *50*, 959–965.

(27) Van Herck, J. L.; De Meyer, G. R.; Martinet, W.; Salgado, R. A.; Shivalkar, B.; De Mondt, R.; Van De Ven, H.; Ludwig, A.; Van Der Veken, P.; Van Vaeck, L.; Bult, H.; Herman, A. G.; Vrints, C. J. Multi-slice computed tomography with N1177 identifies ruptured atherosclerotic plaques in rabbits. *Basic Res. Cardiol.* **2010**, *105*, 51–59.

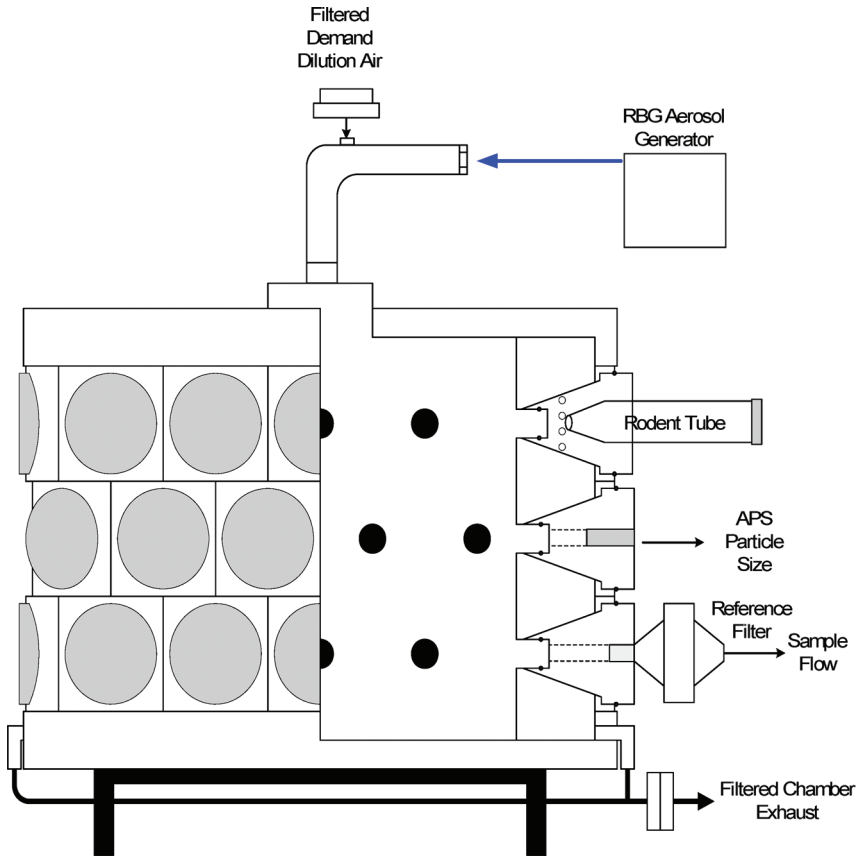

Figure 1. Schematic of the 24-port nose-only rodent inhalation delivery system.

was determined gravimetrically by the difference in weight of filter paper placed on each stage before and after powder deposition. The percent emitted fraction (% EF) was calculated as the total particle mass collected from the stages of the impactor over the total particle mass introduced to the impactor. The fine particle fraction of total dose (FPF_{TD}) was determined as the percentage of aerosolized particles that reached the lower seven stages of the impactor (aerodynamic diameters <5.8 μm) or the lower five stages (aerodynamic diameters <3.3 μm).[28,29] The mass median aerodynamic diameter (MMAD) and geometric standard deviation (GSD) were determined by a linear fit of the cumulative percent less than the particle size range by weight plotted on a probability scale as a function of the logarithm of the effective cutoff diameter.[30,31]

Dry Powder Insufflation and CT Imaging. Male Sprague−Dawley rats (200−250 g; Charles River Laboratories Inc.) were maintained on a 12 h light/dark cycle in humidity and temperature controlled rooms with free water and food access. All animal procedures were conducted according to guidelines approved by The University of Kansas Institutional Animal Care and Use Committee.

Rats were anesthetized by a 67.5 mg/kg ketamine, 3.4 mg/kg xylazine and 0.67 mg/kg acepromazine subcutaneous cocktail. While under anesthesia, rats were placed on a heating pad to maintain a body temperature of 37 °C. The rats were then place in an upright presentation using a stand made in-house for dosing. N1177 NanoCluster (10 mg) was administered by intratracheal insufflation using a Penn-Century DP-4 dry powder insufflator. Powder was delivered through the device using 3 mL of air. At the end of the experiment, the rats were euthanized by isoflurane inhalation overdose. The thoracic cavity was scanned with a Scanco Medical μCT 40 *ex vivo* scanner with a X-ray tube energy of 45 kVp.

Aerosol Inhalation and CT imaging. Male Fischer 344 (F344) rats (125−150 g; Harlan Laboratories, Inc.) were placed in restraint tubes and connected to a 24-port nose-only rodent exposure system (Figure 1). N1177 NanoCluster aerosols were generated with a Palas 1000 rotating brush generator (RBG) with an outlet flow of ∼19 L/min and delivered through a stainless-steel aerosol delivery line into

(28) Lechuga-Ballesteros, D.; Charan, C.; Stults, C. L.; Stevenson, C. L.; Miller, D. P.; Vehring, R.; Tep, V.; Kuo, M. C. Trileucine improves aerosol performance and stability of spray-dried powders for inhalation. *J. Pharm. Sci.* **2008**, *97*, 287–302.

(29) Yang, Z. Y.; Le, Y.; Hu, T. T.; Shen, Z.; Chen, J. F.; Yun, J. Production of ultrafine Sumatriptan succinate particles for pulmonary delivery. *Pharm. Res.* **2008**, *25*, 2012–2018.

(30) Pham, S.; Wiedmann, T. S. Note: dissolution of aerosol particles of budesonide in Survanta, a model lung surfactant. *J. Pharm. Sci.* **2001**, *90*, 98–104.

(31) Vanbever, R.; Ben-Jebria, A.; Mintzes, J. D.; Langer, R.; Edwards, D. A. Sustained release of insulin from insoluble inhaled particles. *Drug Dev. Res.* **1999**, *48*, 178–185.

Table 1. N1177 Particle Size over Time during Media Milling (Values = Average ± SD)

time (min)	particle size (nm)
15	1430 ± 1
30	660 ± 5
45	823 ± 2
60	880 ± 2
90	1068 ± 0.4
120	1200 ± 3

the rodent exposure system with an equivalent exhaust. Rats inhaled the generated aerosols for 21.5 min. Aerosol concentration was measured at the rodent exposure chamber by collection onto preweighed 47-mm Pallflex membrane filters (Type T60A20, Pall Gelman Sciences). Filters were analyzed via differential weight analysis. Particle size was measured at the rodent exposure chamber with an aerodynamic particle sizer (TSI Model 3321) (Figure 1).

Each rat was imaged before and 1 h post exposure on a NanoSPECT/CT (Bioscan, Inc.). An initial whole body topogram was taken to determine the region containing the entire lung volume, with a typical length of ~40 mm. Each image was acquired using the "ultrafine" setting, allowing maximum resolution upon reconstruction. Each acquisition was 6 min long with an X-ray tube energy of 65 kVp and 1000 mA using 240 projections.

CT Data Analysis. CT image analysis was performed by Kitware, Inc. After visual inspection of the scans before and 2 h after dose, the mean Hounsfield unit (HU) density for the full lung parenchyma was measured using a 2D contour drawing tool.

Lung Tissue Toxicity Determination. After CT imaging and animal euthanasia, the lungs were removed and stored in 10% neutral buffered formalin. Tissue samples were taken to a hospital pathology lab for histology processing. Tissue sections representing all depths of the lung were embedded in paraffin wax, and the slices from the tissues were stained with hematoxylin and eosin (H and E) dyes. The results were compared to normal lung histology, and the toxicity results were discussed with a pathologist.

Results and Discussion

N1177 NanoClusters Can Be Successfully Formulated by a Wet Milling Procedure. Since large doses of iodinated contrast agents are typically needed to achieve the minimum required contrast enhancement, a wet milling procedure was selected to formulate the N1177 contrast agent to enable larger batch processing. Using this technique, excipient-free N1177 NanoClusters were successfully created. Formulations containing only the contrast agent without additives reduce the total dose necessary to achieve needed contrast enhancement.

To track the media milling time needed to achieve the appropriate particle size, drug suspension samples were collected at discrete intervals during milling. N1177 particles decreased in size within 30 min followed by an increase in size over 2 h (Table 1). During this process, fine hydrophobic

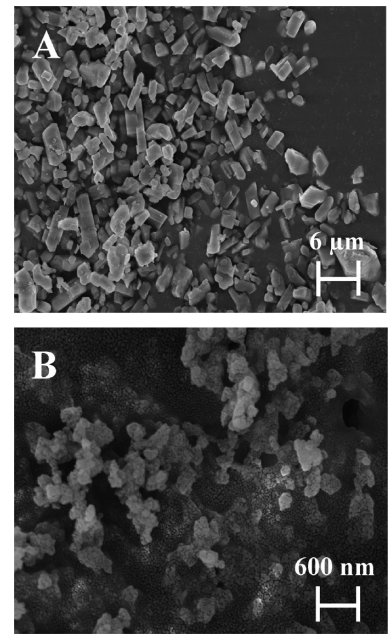

Figure 2. Scanning electron micrographs of N1177 particles: (A) unprocessed N1177 as received and (B) N1177 NanoClusters.

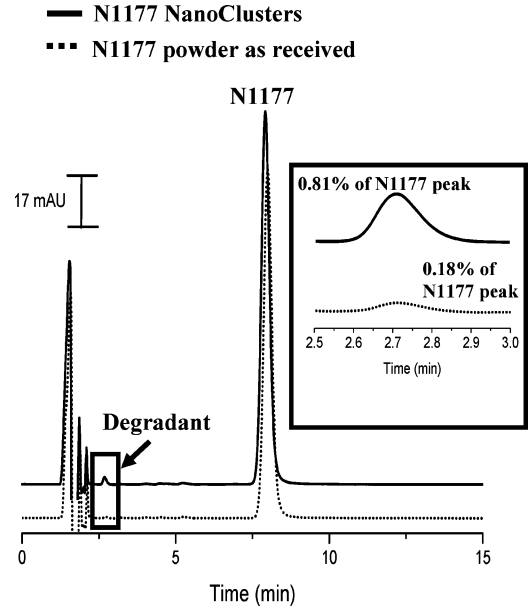

Figure 3. Chromatograms of N1177 NanoClusters compared to N1177 powder as received. The inset highlights the potential degradant peak (retention time = 2.718 min).

nanoparticles were not observed in suspension, but rather assembled into low density agglomerates (i.e., NanoClusters). Particle size, density, and morphology were determined using other techniques.

Scanning electron microscopy revealed differences in the morphology of the unprocessed N1177 powder as received and the N1177 NanoClusters. The unprocessed N1177 appeared as micronized faceted particles (Figure 2A), while images of the NanoClusters showed small nanoparticles (~300 nm) agglomerated into micrometer-sized clusters

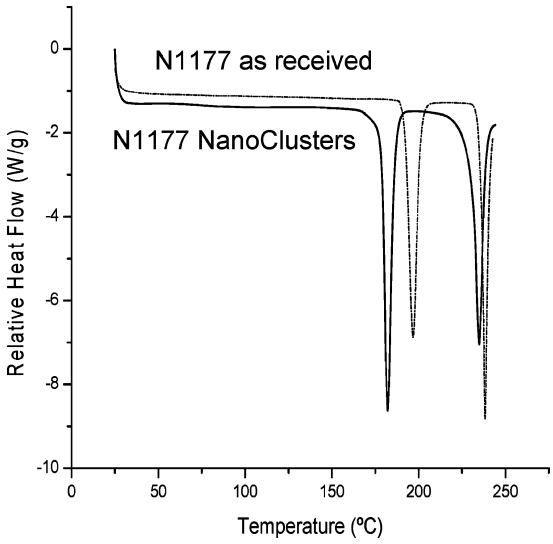

Figure 4. DSC thermograms of N1177 NanoClusters and N1177 powder as received.

Table 2. Particle Size Measured from DLS before and after Low and High Speed Homogenization of N1177 NanoCluster Suspensions (in Pluronic-F127 or DPPC) (Values = Average ± SD)

	particle size (nm)	
	Pluronic-F127	DPPC
before homogenization	1433.4 ± 194.4	847.9 ± 206.5
low speed homogenization	979.2 ± 122.0	781.8 ± 55.3
high speed homogenization	500.3 ± 21.7** [a]	614.7 ± 92.6

[a] $p < 0.05$.

(Figure 2B). Fine nanostructure was retained in the NanoClusters creating a porous matrix that could aid in the aerosolization of the dried particles.

Compound and Particle Stability Are Retained after Formulation into NanoClusters. To verify the chemical stability of N1177 during NanoCluster formulation, HPLC−UV chromatograms of N1177 NanoClusters were compared to N1177 as received (Figure 3). For both NanoClusters and powder as received, N1177 had a retention time of 8.3 min. The only observable difference between the two chromatograms was a 5-fold increase in peak at a retention time of 2.7 min in the NanoCluster chromatogram. This potential degradant peak had a peak area of less than 1% of the N1177 peak. Based on the similarities of the chromatograms, it was concluded that N1177 NanoClusters retained ≥99% of the native structure during the formulation process.

DSC thermograms of N1177 NanoClusters as compared to powder as received showed no differences in the crystalline state of N1177 during the NanoCluster formulation (Figure 4). For the powder as received, an endotherm was observed at 198 °C followed by N1177 degradation at 240 °C. N1177 NanoClusters also exhibited the endotherm characteristic to N1177, but at 182 °C with subsequent compound degradation at 235 °C. This shift in temperature has been observed with other compounds formulated into NanoClusters as well as other types of formulations with reduced particle size.[18,24,32,33] Therefore, it was concluded that the shift in endotherms for N1177 NanoClusters was due to N1177 size reduction during formulation.

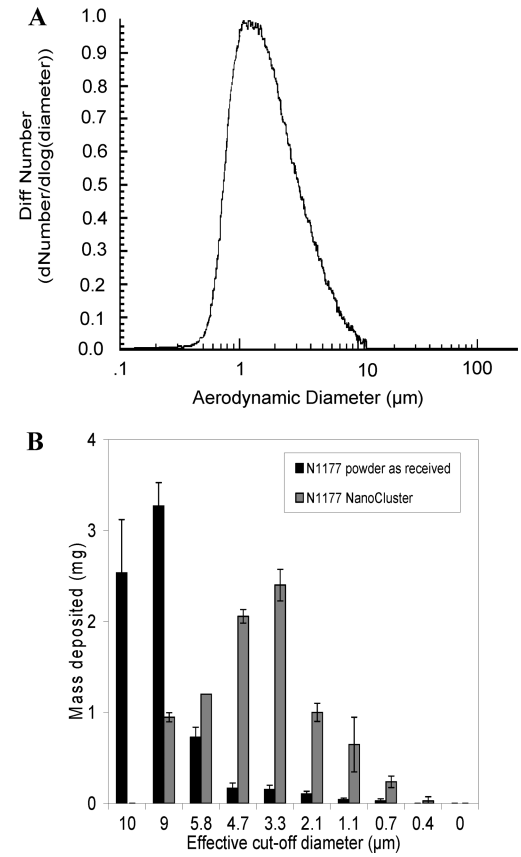

Figure 5. The aerodynamic size distribution of N1177 NanoCluster powder determined by (A) time-of-flight and (B) cascade impaction.

Table 3. Cascade Impaction Results of Lyophilized N1177 NanoCluster Dry Powder (NC) at 30 L/min (Values = Average ± SD)

	N1177	
powder properties[a]	NC	powder as received
% EF[b]	85 ± 5	70 ± 5
% FPF[c]		
<5.7 μm	75 ± 1	7 ± 3
<3.3 μm	22 ± 1	2 ± 1
MMAD (μm)[d]	4.2 ± 0.1	8.6 ± 0.3
GSD[e]	2 ± 0.2	2.3 ± 0.5

[a] At flow rate of ~30 L/min. [b] % EF: Percent emitted fraction. [c] FPF: Fine particle fraction. [d] MMAD: Mass median aerodynamic diameter. [e] GSD: Geometric standard deviation.

NanoCluster particles have the potential to disperse after lung deposition. To probe physical stability, NanoClusters were suspended in Pluronic-F127 surfactant or DPPC and subjected to low and high speed homogenization. DLS measurements of the suspension before and after each homogenization showed no significant difference between the particle size measured before and after low speed homogenization in Pluronic-F127 (Table 2). Under extreme shear (homogenization at 25,000 rpm) the particle size

Figure 6. 3D reconstructed CT images of rat thoracic cavities after 10 mg N1177 NanoCluster dry powder insufflation (A) directly after dose and (B) 2 h post dose. N1177 NanoCluster shown in green and soft tissue shown in pink.

decreased to half the original diameter (Table 2). N1177 NanoClusters suspended in DPPC showed no significant difference in particle size measured under all conditions, which indicated the NanoCluster particles are likely to maintain their microstructure under physiological conditions.

N1177 NanoClusters Have Proper Aerosol Characteristics for Deep Lung Deposition. The aerodynamic size distribution of the N1177 NanoClusters was determined using time-of-flight analysis. The distribution of the NanoClusters was monodispersed (Figure 5A). The median aerodynamic diameter (MAD) was 1.6 μm and 95% of the powder was found to be below 5.3 μm. This data supports that the NanoClusters have the aerodynamic particle size desirable for deposition in the lung periphery. In comparison, the N1177 powder as received showed a MAD of 3.1 μm (data not shown). Therefore, formulating N1177 into NanoClusters resulted in a lower MAD (i.e., a higher fraction of fine particles).

Cascade impaction studies were performed for N1177 NanoCluster powder and compared with that of N1177 powder as received (Table 3). N1177 NanoClusters were mainly deposited in the third stage (3.3 μm). A substantial fraction of fine particles (<5 μm) was observed. N1177 powder as received deposited mainly in the preseparator and zero stage (9.0 μm) (Figure 5B). The high emitted fraction of dry powders obtained at the tested flow rate (~85%) and the results of the fine particle fraction suggested efficient aerosolization of the NanoClusters (Table 2). The mass median aerodynamic diameter (MMAD) of N1177 NanoCluster dry powders was ~4.2 μm. The geometric standard deviation (GSD) was determined from the following equation:[34]

$$\mathrm{GSD} = \left(\frac{d_{84.13\%}}{d_{15.87\%}}\right)^{1/2}$$

where d_n is the diameter at the nth percentile of the cumulative distribution. The GSD was found to be ~2, suggesting particles were relatively monodispersed (Table 2).[18,19]

(32) Tanaka, Y.; Inkyo, M.; Yumoto, R.; Nagai, J.; Takano, M.; Nagata, S. Nanoparticulation of poorly water soluble drugs using a wet-mill process and physicochemical properties of the nanopowders. *Chem. Pharm. Bull. (Tokyo)* **2009**, *57*, 1050–1057.

(33) Trasi, N. S.; Boerrigter, S. X.; Byrn, S. R. Investigation of the milling-induced thermal behavior of crystalline and amorphous griseofulvin. *Pharm. Res.* **2010**, *27*, 1377–1389.

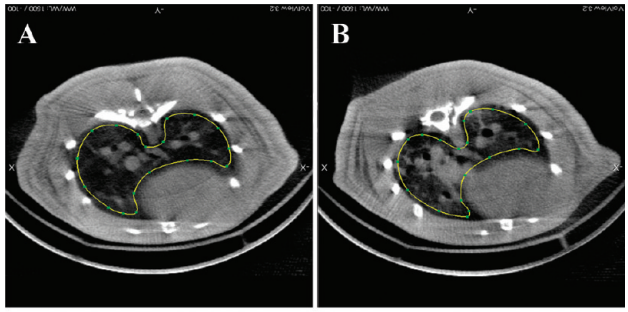

Figure 7. CT image transverse cross sections of rat lungs (A) before dose and (B) after N1177 NanoCluster aerosol inhalation. The region of interest used for calculating contrast is outlined.

Aerosolization of N1177 NanoClusters Offers Lung Contrast Enhancement. Local delivery of N1177 NanoClusters by dry powder insufflation into rats dramatically enhanced image contrast of the lung airways. The trachea and bronchi were clearly seen in the 3D reconstructed CT images taken directly after insufflation (Figure 6A). More importantly, visualization of the respiratory bronchioles and some alveolar structures in the lung periphery were evident, confirming deep lung deposition of the NanoClusters. After 2 h (Figure 6B), the contrast agent cleared from the central airways with contrast more localized to the trachea or lung periphery. This suggested that the compound may be further concentrating in the lung periphery over the course of 2 h. Although a large portion of the dose was visibly deposited in the trachea after insufflation, visualization of the entire airway was improved with the N1177 NanoClusters. It is important to note that insufflation delivery was performed by quickly forcing a burst of 3 mL of air through the insufflator device which then dispensed the compound into the lungs. With this method, compound was forcibly delivered to the lungs with favored deposition to the right lung due to anatomical positioning, branching to the right lung being more vertically aligned. This delivery technique, therefore, is not representative of compound deposition in the lung after aerosol inhalation and may account for some of the observed powder in the upper respiratory tract and enhanced contrast in the right lung.

To better aerosolize the N1177 NanoClusters using a more clinically relevant delivery method, pulmonary delivery was conducted using passive, nose-only inhalation of generated aerosols (Figure 1). Aerosol concentrations measured at the rodent exposure chamber showed 1.04 mg/mL N1177 NanoClusters were maintained in the chamber and delivered to the rats for 21.5 min. Particle size measurements by dynamic light scattering revealed that the generated aerosols had a MAD of 1.1 μm (GSD = 1.6) within the aerosolization chamber. Analysis of the CT images revealed a 118 HU difference between the images taken prior to dosing (−620 HU) and 1 h post inhalation (−502 HU) (Figure 7). This excellent contrast enhancement was well above the 30 HU minimum needed for contrast.[8] Lower doses could potentially be explored to reduce the amount of N1177 was administered to achieve adequate contrast.

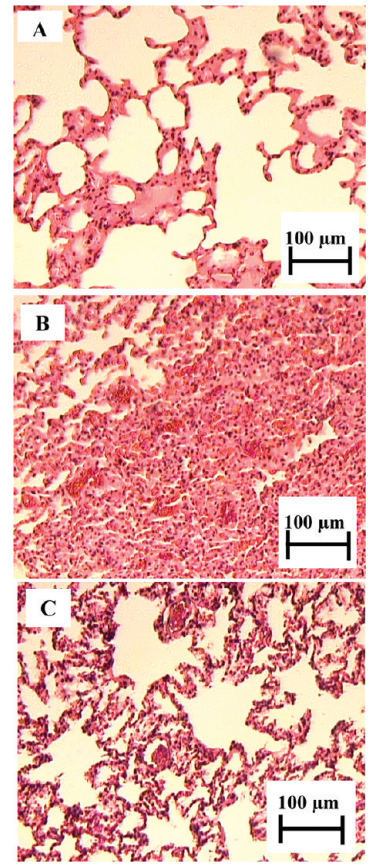

Figure 8. Rat lung tissue histology (A) 2 h after aerosol inhalation of N1177 NanoClusters, (B) 2 h after insufflation of N1177 NanoClusters, and (C) normal lung tissue.

N1177 NanoClusters Exhibited No Acute Lung Toxicity When Inhaled. Several sections of lung tissue representing all depths of the lung were sliced for histological examination. Lung tissue from the aerosol inhalation studies revealed no inflammatory response from the N1177 NanoClusters (Figure 8A). In comparison to normal lung tissue (Figure 8C), no differences were observed and an increase in macrophages was not evident. Lung tissue histology from rats dosed by dry powder insufflation revealed a mild hemorrhagic response (Figure 8B). This response was most likely due to the focal deposition of highly concentrated contrast agent in discrete lung regions. During the insufflation method, N1177 was propelled at high doses into confined regions whereby the large amounts of contrast agent most likely elicited the inflammatory response. Although there were regions of inflammation after insufflation, the majority of the lung tissue presented no inflammatory response. Accompanying the hemorrhagic response was the presence

(34) Fiegel, J.; Garcia-Contreras, L.; Thomas, M.; VerBerkmoes, J.; Elbert, K.; Hickey, A.; Edwards, D. Preparation and in vivo evaluation of a dry powder for inhalation of capreomycin. *Pharm. Res.* **2008**, *25*, 805–811.

of macrophage clusters in the alveolar sacs. Previously, studies of N1177 nanoparticles showed macrophage uptake after iv administration followed by transit to regional lymph nodes.[25–27] It is probable, therefore, that alveolar macrophage clusters present in the lung after insufflation may transport N1177 to lung lymph nodes. For both delivery methods, the effects of N1177 NanoClusters over a longer period of time will be important to determine inflammation and to better characterize the regional transport of N1177.

Conclusions

Aerosolized contrast media may provide a noninvasive means to localize contrast agents to the lungs to improve thoracic CT imaging accuracy for lung disease and damage diagnosis. Deposition of contrast agents to the lung periphery, however, can be complicated by formulations with undesirable aerosol performance. In this study, a diatrizoic acid derivative, N1177, was formulated using NanoCluster technology, a unique and simple method to create an inhalable, excipient-free dry powder contrast agent. Particle characterization revealed that the NanoClusters had desirable aerosol characteristics and offered a fine particle fraction suitable for deposition in the lung periphery. After pulmonary delivery to rats, a substantial contrast enhancement of 118 HU was achieved. Additionally, lung tissue histological examination revealed that no acute lung toxicity was associated with the N1177 NanoClusters after inhalation. Overall, the N1177 NanoClusters were capable of deposition in the lung periphery with exceptional contrast enhancement for lung visualization by thoracic CT imaging.

Acknowledgment. The authors would like to gratefully acknowledge Savara Pharmaceuticals for funding and NanoScan, Inc., for providing N1177. Additional lab funding was provided by The Cystic Fibrosis Foundation, The Coulter Foundation, The Higuchi Biosciences Center, The American Heart Association, NIH (R03 AR054035, P20 RR016443 and T32 GM08359-11) and The Department of Defense. Special thanks to Dr. Valentin David (University of Kansas Medical Center) for 3D CT reconstruction, Dr. Rick Avila (Kitware, Inc.) for CT image analysis, Dr. Mike Thompson (Lawrence Memorial Hospital) for histology processing and consultation, Dr. C. Russell Middaugh (University of Kansas) for equipment use, The University of Kansas Microscopy Lab for SEM assistance. Small-animal CT images in this article were generated at the Keck-UNM Small-Animal Imaging Resource (KUSAIR) established with funding from the W.M. Keck Foundation, and supported by NCI Cancer Center Support Grant (P30CA118100-06).

MP1000718